



Crystal Structure Analysis of Lithium Zirconate Prepared from Local Sand at a various ratio of Li_2CO_3 to ZrO_2

V. Natalia^{1,2}, F. Rahmawati^{2*}, A. Purwanto³

¹Department of Chemistry, Master Program Graduate School, Sebelas Maret University, Jl. Ir. Sutami 36 A, Surakarta, 57126

²Research Group of Solid State Chemistry & Catalysis, Department of Chemistry, SebelasMaret University, Jl. Ir. Sutami 36 A, Surakarta, Indonesia 57126

³Research Group of Battery Development, Department of Chemical Engineering, SebelasMaret University, Jl. Ir. Sutami 36 A, Surakarta, Indonesia 57126

Received 13 May 2017,
Revised 16 Nov 2017,
Accepted 19 Nov 2017

Keywords

- ✓ Lithium zirconate,
- ✓ Zircon sand,
- ✓ Crystal structure,
- ✓ Solid state,
- ✓ Zirconiumdioxide.

fitria@mipa.uns.ac.id ;
Phone: +62271776629;
Fax: +62271776629

Abstract

Lithium zirconate, Li_2ZrO_3 is a promising candidate anode material for lithium ion battery. Due to the abundant of zircon sand as a raw material for lithium zirconate synthesis in Indonesia, therefore this research study the preparation of lithium zirconate. The aims are to increase the economic value of the local zircon sand as well as to ensure the functional materials supply for developing energy conversion technology. The Lithium zirconate, Li_2ZrO_3 was prepared by solid state reaction with Li_2CO_3 and ZrO_2 from zircon sand as starting materials. The produced white powder was then analyzed by XRD to ensure the result by comparing with a standard diffraction. Furthermore, the crystal structure was also determined by conducting refinement on the diffraction data. The refinement proceeded well with the Le Bail method in a RIETICA software. The crystal structure is monoclinic with a space group of $C21/c1$. The cell parameters are $a = 5.4304 \text{ \AA}$, $b = 9.0240 \text{ \AA}$, and $c = 5.4207 \text{ \AA}$. The structure compatibility is shown by the low R_p and R_{wp} , i.e. 6.78% and 7.17%, respectively. This research also found that the prepared lithium zirconate is in a single phase without any impurities presence. The Fourier plot of electron mapping shows a significant change on electron map when the material converted from ZrO_2 to Li_2ZrO_3 . The FTIR spectra shows differences in the adsorption peaks of ZrO_2 and Li_2ZrO_3 . Meanwhile, the particle size of Li_2ZrO_3 particles is around 1.1 – 2.1 μm .

1. Introduction

Lithium-Ion rechargeable batteries (LIBs) have good reversibility and high power density [1]. Electrode materials for rechargeable lithium-ion batteries is an important part for development of energy storage system [2]. Among some materials, Lithium zirconate, Li_2ZrO_3 is of a particular interest for anode materials due to the good structural stability and high lithium diffusion coefficients. The change of the unit cell volume is only ~0.3% during discharge or charge process [3]. The Li_2ZrO_3 itself is a stable chemical compound and inert in some common non-aqueous electrolytes. It is also suitable for coating shell to protect the electrode material [4]. The Li_2ZrO_3 also can coat $\text{Li}_4\text{Ti}_5\text{O}_{12}$ (LTO) without disturbing the intrinsic structure of LTO [5]. In other research, the Li_2ZrO_3 layer was coated on the surface of silicon/graphite/carbon materials and it was proven to stabilize the electrode through the formation of a stable and a compact solid electrolyte interface (SEI) layer on the electrode surface [6].

The crystalline Li_2ZrO_3 consists of two phases namely tetragonal $t\text{-Li}_2\text{ZrO}_3$ and monoclinic $m\text{-Li}_2\text{ZrO}_3$. The $t\text{-Li}_2\text{ZrO}_3$ can undergo phase changing at 1173 K to stable $m\text{-Li}_2\text{ZrO}_3$ [7]. Li_2ZrO_3 has been synthesized by different methods such as combustion method [8], citrate sol-gel [9], solid state reaction [3,5], etc. Solid state reaction is a chemical reaction synthesized without solvent requirement. This method has some advantages, such as simple to handle, reduce pollution, and low cost [10]. The synthesis of Li_2ZrO_3 was also successfully conducted by a conventional solid state reaction with a commercial ZrO_2 and Li_2CO_3 as starting materials. X-ray diffraction analysis equipped with a crystal structure refinement shows that the produced Li_2ZrO_3 is a single phase with a monoclinic structure and $C12/c1$ of space group [3]. The monoclinic Li_2ZrO_3 can also be synthesized from a lithium carbonate, zirconia, and potassium carbonate mixture with the

temperature range of 850 – 1200 °C [11]. The result shows that below those temperature range, the reaction to form the lithium zirconate did not proceed, meanwhile above those temperature range, the volatilization of Li₂O occurred.

ZrO₂, as a raw material, is the main component to prepare the lithium zirconate as electrode for Lithium ion battery. Our previous study found that the ZrO₂ successfully can be synthesized from a concentrate zircon sand through a caustic fusion method. The produced ZrO₂ powder crystallized in a tetragonal structure and space group of *P42/nmc* [12]. On the other research, the ZrO₂ is also developed as a material for fuel cell [13] and semiconductor photocatalyst [14]. Zircon sand is a side product of tin mining plant with low economic value. Due to a high abundance of this zircon sand in Indonesia, therefore an effort to prepare an electrode material, Li₂ZrO₃, from the zircon sand become an interesting subject. In this research, the Li₂ZrO₃ was prepared by solid state reaction with ZrO₂ from zircon sand as the raw material. The Li₂ZrO₃ was prepared at a various ratio of ZrO₂ and Li₂CO₃. The produced materials were then analyzed to understand the effect of ratio of Li source, the Li₂CO₃, to the raw ZrO₂ material on its crystal structure and its cell parameters.

2. Material and Methods

2.1. Synthesis of material

Li₂ZrO₃ materials were synthesized by solid state reaction using Li₂CO₃ and ZrO₂ as starting materials. ZrO₂ has prepared by caustic fusion from zircon sand through decomposition, leaching, and co-precipitation process [12]. The prepared ZrO₂ and Li₂CO₃ were mixed at a various mol ratio of 1:1, 1:1.05, and 1:1.075. The mixing process was done in a ball mill at 300 rpm for 2 hours, with zirconia balls as crusher. Ball mill process was then continued to 480 rpm for 2 hours. The mixture then was calcined at 950 °C for 10 hours to produce Li₂ZrO₃ and cooled at room temperature [3].

2.2. The analysis of material

XRD pattern at room temperature for the sample was recorded by Rigaku MiniFlex 600 X-ray diffraction instrument with CuK α radiation ($\lambda=1.5406$ Å). The intensities were recorded in the 2 θ ranges between 10-80°. The diffraction data were refined with Le Bail method by a RIETICA software (a free edition) to study its crystallinity, cell parameters and electron density mapping. The peak profiles were modeled using pseudo-Voigt peak shape. Other experimental parameters refined were the instrument zero, scale factor, the lattice parameters, and the peak shape parameters $u, v, w, \gamma_0,$ and γ_1 [15]. The parameters which were inputted to the software for conducting refinement are listed in Table 1.

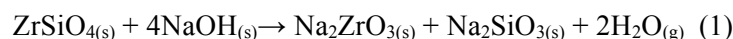
Table 1: The Crystal parameters that was used for data input in refinement. The parameters is from ICSD#94895 as the result Le Bail refinement with the crystal name of monoclinic.

Cell parameters	Li ₂ ZrO ₃
Space group	<i>C12/c1</i>
a (Å)	5.4240 (1)
b (Å)	9.0263 (2)
c (Å)	5.4197 (1)
$\alpha=\gamma$	90
β	112.701 (1)
Z	4

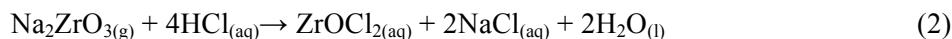
FTIR analysis was measured by Shimadzu Infrared Prestige 21 with a KBr pellets as substrate and provided 45 scans and 2 resolutions. It was conducted to investigate the functional groups existed and specifically identify structure in the prepared materials [16]. Meanwhile, SEM analysis (FEI Inspect s50) was used to investigate the surface morphology, the form and to estimate the particle size of the Li₂ZrO₃.

3. Results and discussion

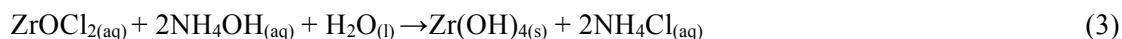
The reaction of ZrO₂ formation from zircon sand using caustic fusion [12] are listed in equation (1), (2), (3), (4), and (5) as it was proposed by El Barawy et al. [17].



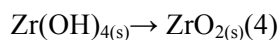
During acid leaching with HCl solution, sodium zirconate dissolve into this strong HCl acid solvent to form zirconium perchlorate.



The next process was to precipitate zirconium hydroxide by add an ammonium hydroxide solution into zirconium perchlorate solution.



Zirconium hydroxide then was heated at 800 °C for 5 hours to form zirconium dioxide, ZrO_2 .



XRD pattern of the prepared ZrO_2 (Figure 1) shows that the peaks at 2θ of 30.074°, 60.028°, and 62.58° are in agreement with the standard diffraction of ZrO_2 ICSD#66787. However, the peaks are broader than the peaks in standard ICSD#66787. It indicates that the prepared zirconia from zircon sand has lower crystallinity than the commercial ZrO_2 also occurred previously [12].

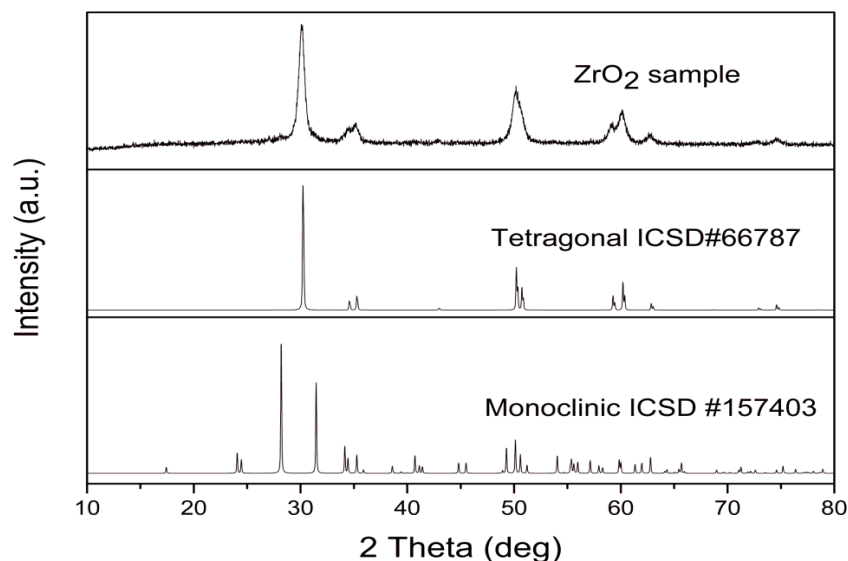


Figure 1: The diffraction pattern of the prepared ZrO_2 in comparison with the standart diffraction of tetragonal ZrO_2 ICSD #66787 and monoclinic ZrO_2 ICSD#157403.

The XRD patterns of the prepared Lithium zirconate at a various composition in comparison with Li_2ZrO_3 diffraction standard ICSD#94895(Figure 2).From Figure 2(a) and (b), we observed that the Lithium zirconate was synthesized at ratio of $\text{ZrO}_2:\text{Li}_2\text{CO}_3 = 1:1$ and $1: 1.05$ still contain of the ZrO_2 phase that appear at 2θ of 23.93° and 28.08°.

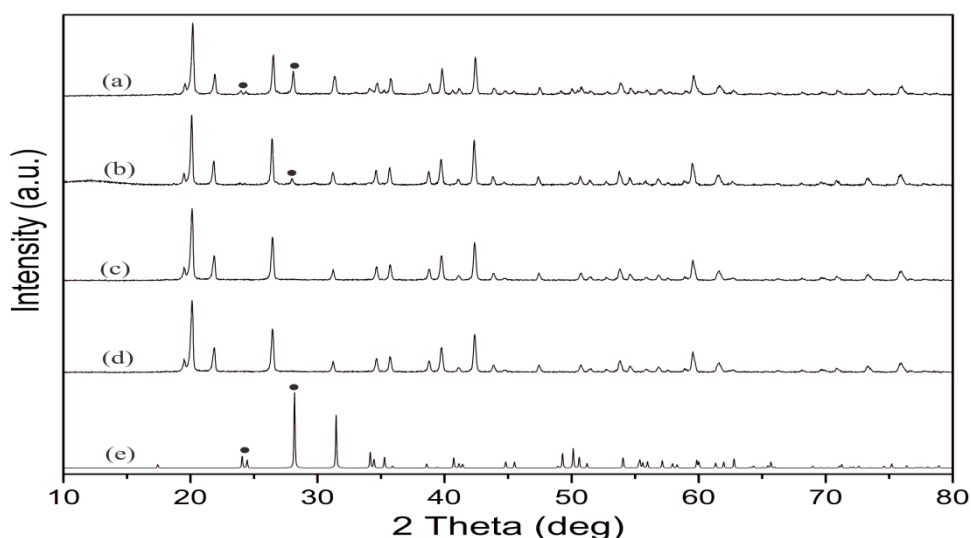
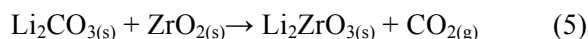


Figure 2: Diffraction patterns of the Li_2ZrO_3 samples synthesized using different amount of $\text{ZrO}_2: \text{Li}_2\text{CO}_3$, (a)1:1; (b) 1:1.05; (c) 1:1.075 with its comparison to standard diffraction of (d) Li_2ZrO_3 monoclinic ICSD #94895 and (e) the monoclinic ZrO_2 ICSD#157403. The sign • refers to the monoclinic ZrO_2 peak.

Meanwhile, when the Li_2CO_3 content increased up to 7.5%, the diffraction pattern become single phase of Li_2ZrO_3 without the presence of other phases in Figure 2(c). The diffraction patterns of the prepared Li_2ZrO_3 show sharp peaks indicating high crystallinity product of the solid state reaction that follow a reaction as stated by Pfeiffer and Knowles [18].



XRD data of the prepared Li_2ZrO_3 were refined with Le Bail method, and the refinement result found that the crystal structure of the prepared lithium zirconate is monoclinic. Different composition resulted the same crystal structure and space group i.e., $C21/c1$. The cell parameters are listed in Table 2. Meanwhile, the Le Bail plots are described in Figure 3. The Le Bail plots of the prepared Li_2ZrO_3 that was produced at ratio of ZrO_2 and Li_2CO_3 1:1 and 1:1.05 in Figure 3(a) shows high green peaks at 2θ of 23.93° and 28.08° . Green curve is confirming the difference between experiment data and the calculation data. The peaks at 23.93° and 28.08° are identified as monoclinic ZrO_2 . When the content of Li_2CO_3 increased up to 7.5% or the ratio of $\text{ZrO}_2:\text{Li}_2\text{CO}_3$ is 1:1.075, the green peaks at 2θ of 23.93° and 28.08° disappear and the material became a single phase of Li_2ZrO_3 in Figure 3(b). The refinement compatibility with single Li_2ZrO_3 phase is shown by low residual value, i.e., R_{wp} 7.17%.

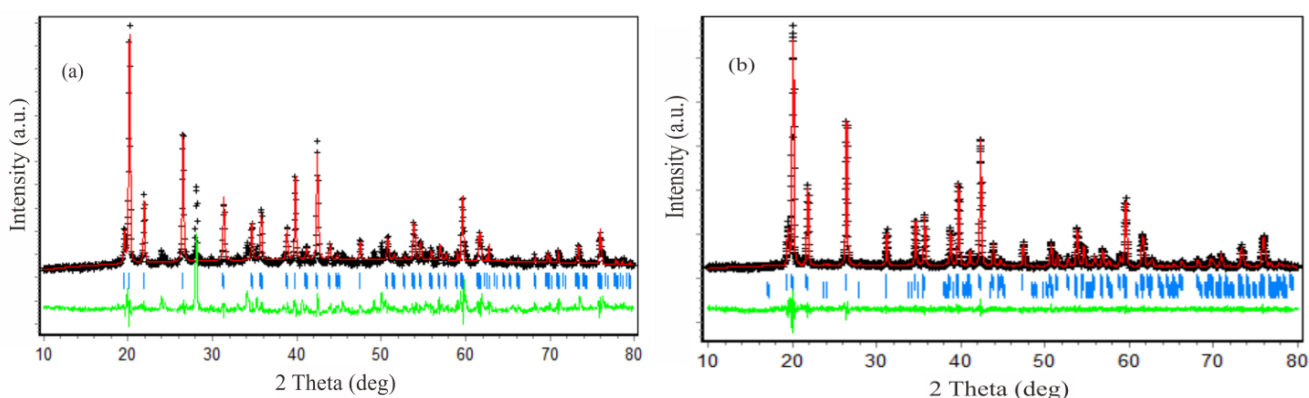


Figure 3: The Le Bail plots of Li_2ZrO_3 sample synthesized using amount of $\text{ZrO}_2 : \text{Li}_2\text{ZrO}_3 =$ (a) 1:1 and (b) 1:1.075 with monoclinic Li_2ZrO_3 ICSD#94895. (+ : experiment data, - : calculation result, - : differences between experiment data and calculation data, - : bragg position).

Table 2: Cell parameters and crystal structure of the synthesized ZrO_2 and Li_2ZrO_3 .

Cell parameters	Crystal structure			
	ZrO_2	Li_2ZrO_3 (1:1)	Li_2ZrO_3 (1:1.05)	Li_2ZrO_3 (1:1.075)
	Tetragonal	Monoclinic	Monoclinic	Monoclinic
	$P421NMC$	$C21/c1$	$C21/c1$	$C21/c1$
a (Å)	3.5978(7)	5.4367(9)	5.4280(6)	5.4304(3)
b (Å)	3.5978(7)	9.0378(4)	9.0324(3)	9.0240(6)
c (Å)	5.1901(7)	5.4208(4)	5.4249(8)	5.4207(1)
V (Å ³)	67.18(5)	245.69(3)	245.30(2)	245.01(4)
α	90	90	90	90
β	90(1)	112.72(1)	112.74(1)	112.72(7)
γ	90	90	90	90
R_p (%)	6.84	13.89	8.43	6.78
R_{wp} (%)	8.76	17.91	11.22	7.17
χ^2	1.1	2.06	2.27	0.55

The Fourier plots of the electron density of ZrO_2 and Li_2ZrO_3 at x, y and z axis are described in (Figure 4, 5 dan 6), respectively. The plots in particular of ZrO_2 at the x, y and z axes show few a different pattern indicating the presence of impurities. The presence of impurities were also found on our previous study, such as Na_2O

14.71%, SiO₂ 3.03%, MgO 2.56%, etc [12], and those impurities may affect the electron distribution. While, the plots show a significant change on electron map when the material converted from ZrO₂ to Li₂ZrO₃. The distance between ions and cell parameters were also changed, confirmed by result refinement (Table 2).

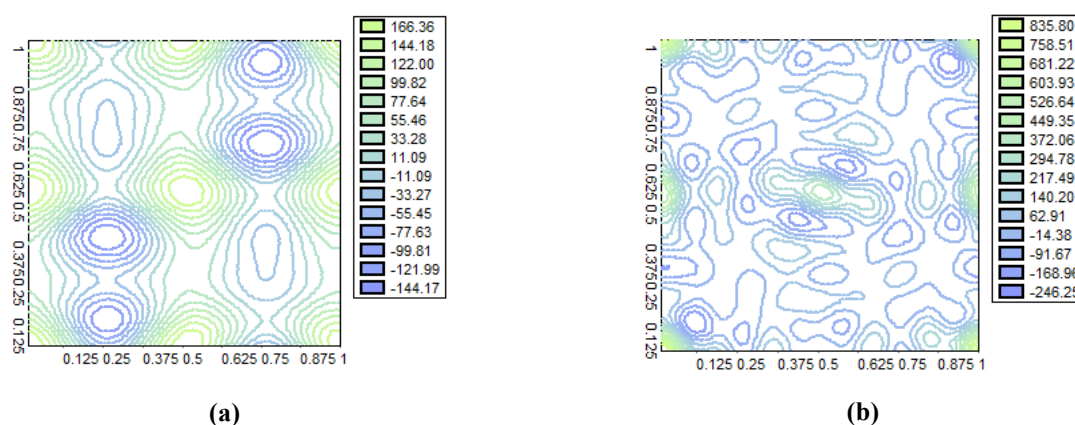


Figure 4: The Fourier plot of electron density at X axes (slice 1) in (a) ZrO₂ and (b) Li₂ZrO₃.

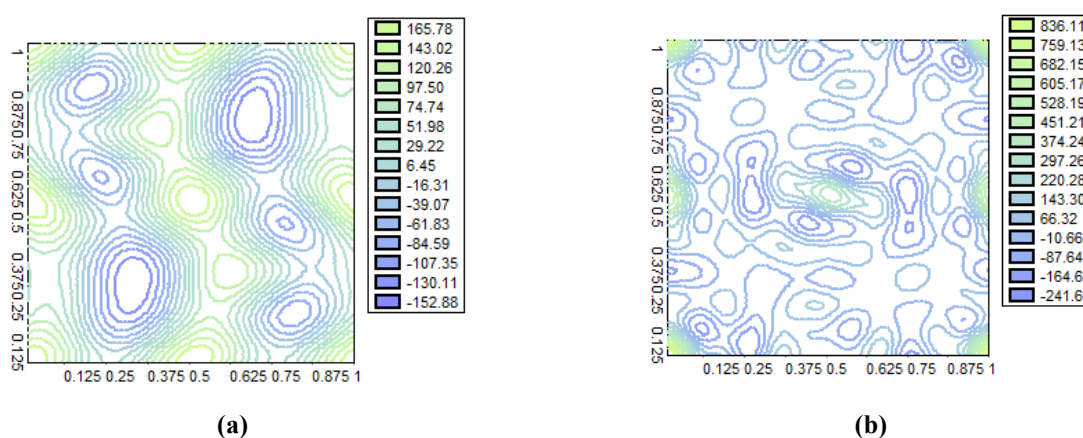


Figure 5: The Fourier plot of electron density at Y axis (slice 1) in (a) ZrO₂ and (b) Li₂ZrO₃.

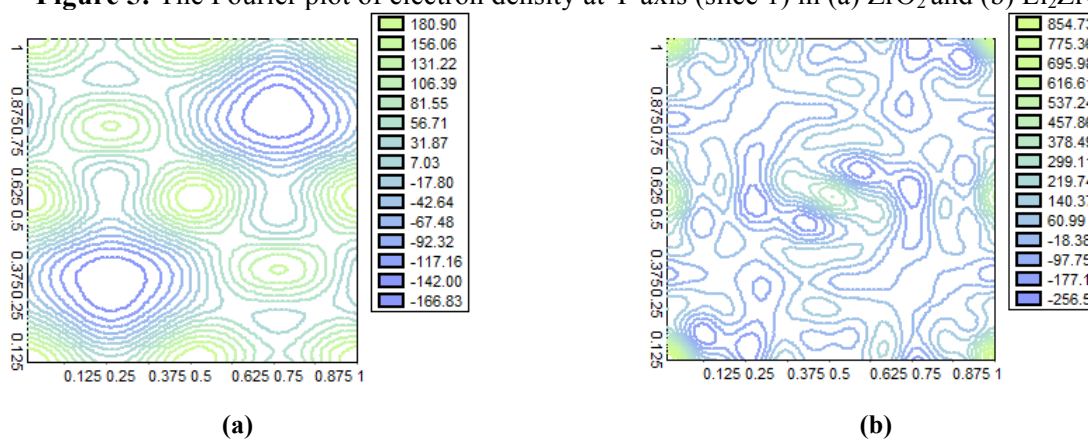


Figure 6: The Fourier plot of electron density at Z axes (slice 1) in (a) ZrO₂ and (b) Li₂ZrO₃.

The formation of ZrO₂ and Li₂ZrO₃ was analyzed by FT-IR and produced spectrum as depicted in Figure 7. The FT-IR in Figure 7(a) shows a characteristic broad peak at wavenumber of 3426.62 and 2904.92 cm⁻¹. It indicates the presence OH stretching due to the absorption and co-ordination of water, Zr-OH [19,20,21]. The peak around 1600 cm⁻¹ is assigned to the water bending mode [19]. The absorption at 744.55, 501.51, and 420.5 cm⁻¹ correspond to the Zr-O stretching band [21,22]. Meanwhile, in Figure 7(b) there are peaks at 1529.62 and 1448.6 cm⁻¹ which indicates the presence of carbonate remaining from preparation [23]. The two following peaks at 753.23 and 576.74 cm⁻¹ correspond to ZrO₃²⁻ ion [24]. The Li-O vibration appears at 443.66 cm⁻¹ agreement with experimental below *ca.* 500 cm⁻¹ where the Li-O vibration are active [25].

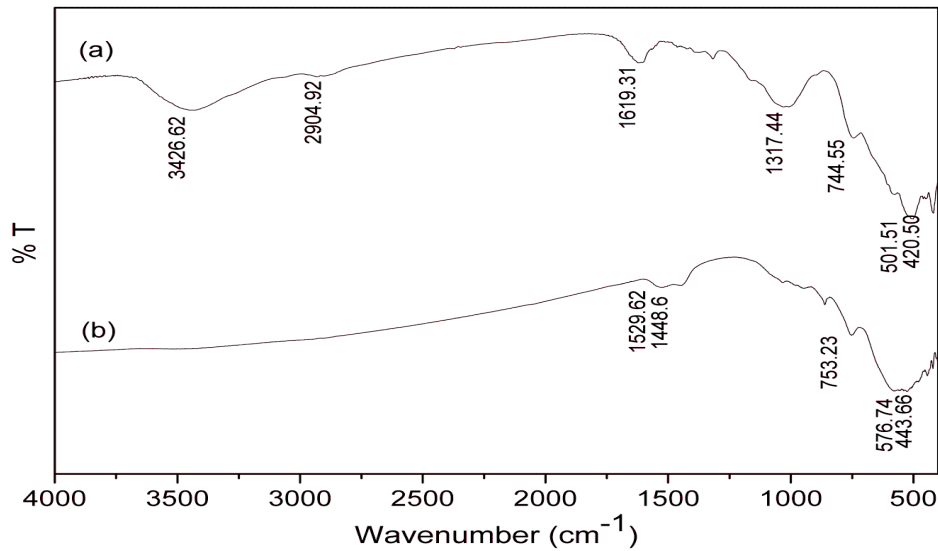


Figure 7: FT-IR spectrum of ZrO_2 (a) and Li_2ZrO_3 (b).

Morphological aspect of the synthesized Li_2ZrO_3 sample were investigated by SEM analysis. Figure 8(a), (b) and (c) shows SEM images of Li_2ZrO_3 sample at different magnifications. The particles are on a heterogeneous size ranging from 1.1 – 2.1 μm , with the most probable size at 1.5 μm (Figure 8(d)). Sintering at high temperature may cause particle agglomeration to form a size larger than 1 μm [10].

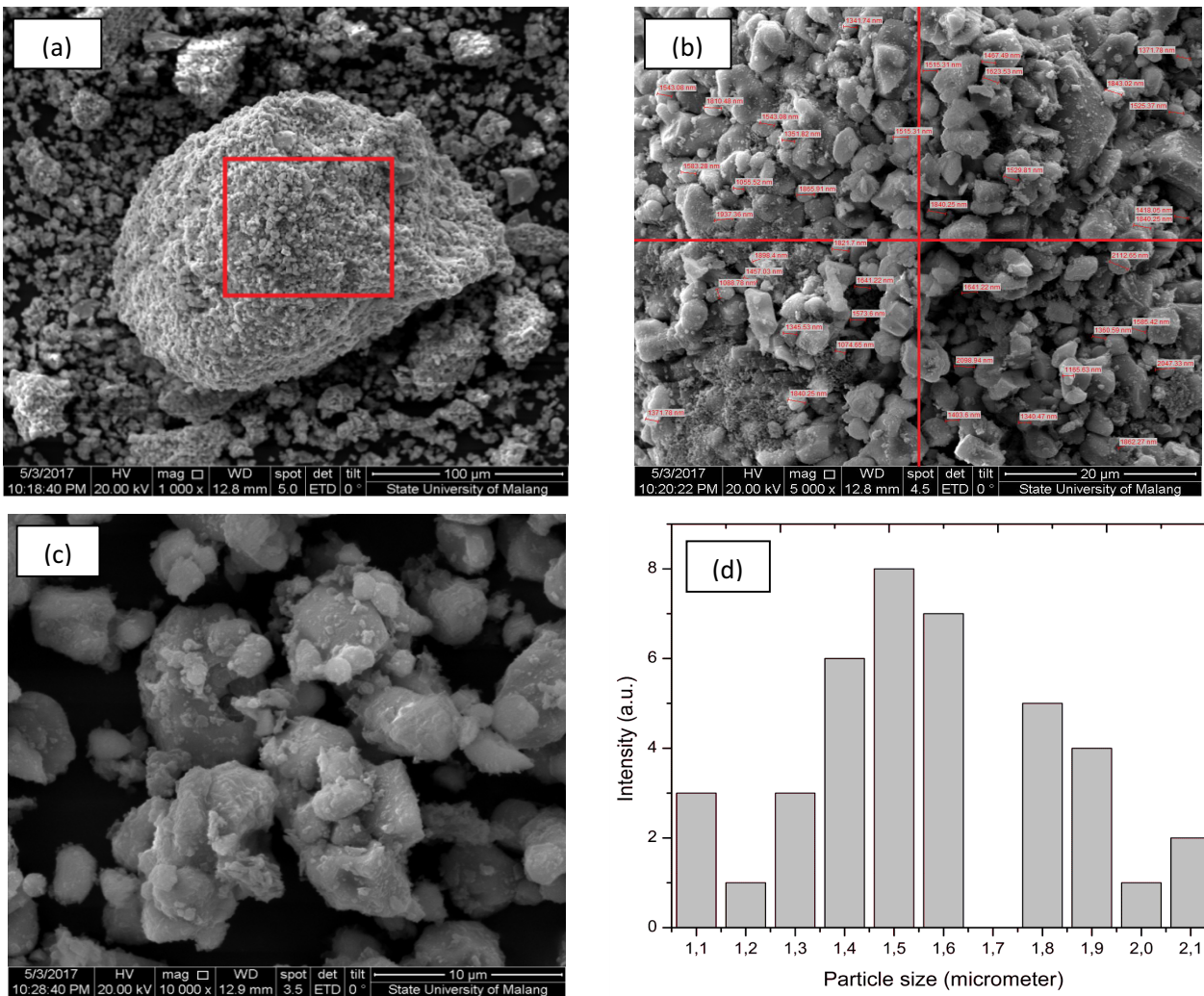


Figure 8: Scanning electron micrographs of Lithium zirconate, Li_2ZrO_3 prepared $ZrO_2 : Li_2CO_3 = 1 : 1.075$ at $900\text{ }^\circ C$ (a) magnification 1000 x, (b) 5000 x, (c) 10000 x, and (d) histogram of distribution of average particle size of the Li_2ZrO_3 particles.

Conclusion

Lithium zirconate, Li_2ZrO_3 powder was successfully synthesized from ZrO_2 , which prepared from local zircon sand by solid state reaction. Li_2ZrO_3 pattern is in a single phase without any impurities presence. The crystal structure is monoclinic with space group of $C21/c1$. The cell parameters are $a= 5.4304\text{\AA}$, $b= 9.0240\text{\AA}$, and $c= 5.4207\text{\AA}$. The Fourier plot of electron mapping shows a significant change on electron map when the material converted from ZrO_2 to Li_2ZrO_3 . The FTIR spectra shows differences in the adsorption peaks of ZrO_2 and Li_2ZrO_3 . The synthetic method to produced a Li_2ZrO_3 forming particles with a diameter about 1.1 – 2.1 μm .

Acknowledgments-This research is a part of Hibah Mandatory 2017 funded by PNPB SebelasMaret University. Authors express gratitude for the support.

References

1. M. El Joumani, S. Bououd, Z. El Abbassi, F. Saidi, A. Kafih, A. El Hourch, *J. Mater. Environ. Sci.* 8 (2017) 188.
2. B. Dunn, H. Kamath, J. Tarascon, *Science* 334 (2011) 928.
3. Y. Dong, Y. Zhao, H. Duan, J. Huang, *Electrochim. Acta* 161 (2015) 219.
4. J. Ni, H. Zhou, J. Chen, X. Zhang, *Electrochem. Acta* 53 (2008) 3075.
5. H. Zhang, Y. Liu, T. Wang, Y. Yang, S. Shi, G. Yang, *Appl. Surf. Sci.* 368 (2016) 56.
6. M. Li, M. Qu, X. He, Z. Yu, *J. Power Sources* 188 (2009) 546.
7. S. Wang, C. An, Q.H. Zhang, *J. Mater. Chem. A* 1 (2013) 3540.
8. D. Cruz, H. Pfeiffer, S. Bulbulian, *Solid State Reaction* 8 (2006) 470.
9. Q. Xiao, Y. Liu, Y. Zhong, W. Zhu, *J. Mater. Chem.* 21 (2011) 3838.
10. H.M. Marvaniya, K.N. Modi, D.J. Sen, *Int. J. Drug Dev& Res* 3 (2011) 42.
11. J. Ida, R. Xiong, Y.S. Lin, *Sep. & Pur Tech.* 36 (2004) 41.
12. F. Rahmawati, I. Permadani, S. Soepriyanto, D.G. Syarif, E. Herald, *Double Steps Leaching and Filtration in Caustic Fusion Method to Produce Zirconia from Local Zircon Concentrate-2015*, in 2014 International Conference of Physics and Its Applications, Atlantis Press, pp. 99-102.
13. F. Rahmawati, B. Prijamboedi, S. Soepriyanto, Ismunandar, *Int. J. Min. Metall. Mater.* 19 (2012) 863.
14. I. Permadani, D.A. Phasa, A.W. Pratiwi, F. Rahmawati, *Bull. Chem. React. Eng. & Catal.* 11 (2016) 133.
15. V.K. Peterson, *Powder Diffraction* 20 (2005) 14.
16. A.-H. El Foulani, A. Aamouche, A. Jedaa, M. Amjoud, K. Ouzaoult, *J. Mater. Environ. Sci.* 8 (2017) 863.
17. K.A. El Baraway, S.Z. El Tamil, A.A. Francis, *T I Min Metall C* 109 (2000) 49.
18. H. Pfeiffer, K.M. Knowles, *J. Eur. Ceram. Soc.* 24 (2004) 2433.
19. E.A. Faria, J.S. Marques, I.M. Dias, R.D.A. Andrade, P.A.Z. Suarez, A.G.S. Prado, *J. Braz. Chem. Soc.* 20 (2009) 1732.
20. S. Jothi, N. Prithivikumar, N. Jeyakumar, *Characterization of Zirconium Oxide Thin Films Prepared by Sol-Gel Method*, in International Conference on Materials and Characterization Techniques, pp. 1971-1973.
21. S. Su, M. He, N. Zhang, C. Cui, *Analytical Methods* 6 (2014) 1182.
22. V.R. Chinchamalpure, S.M. Chore, S.S. Patil, G.N. Chaudhani, *Analytical Methods* 6 (2014) 1182.
23. Y. Zhou, A. Petric, *J. Electrochem. Soc.* 140 (1993) 1388.
24. G. Socrates, *Infrared and Raman Characteristic Group Frequencies: Table and Charts*, John Wiley & Son, Ltd, Chichester, Third Edition, 2001.
25. C.P.E. Varsamis, A. Vegiri, E.I. Kamitsos, *Condensed Matter Physics* 4 (2001) 119.

(2018) ; <http://www.jmaterenvironsci.com>